Insights into the Electronic Structure of the Oxygen Species Active in Alkene Epoxidation on Silver

Travis E. Jones,*[†,‡] Tulio C. R. Rocha,[‡,§] Axel Knop-Gericke,[‡] Catherine Stampfl,[¶] Robert Schlögl,[‡] and Simone Piccinin[†]

[†]CNR-IOM DEMOCRITOS, c/o SISSA, via Bonomea 265, I-34136 Trieste, Italy
[‡]Department of Inorganic Chemistry, Fritz-Haber-Institut der Max-Planck-Gesellschaft, Faradayweg 4-6, 14195 Berlin, Germany
[¶]School of Physics, The University of Sydney, Sydney, New South Wales 2006, Australia

S *Supporting Information*

ABSTRACT: Extensive density functional theory calculations of the O_{1s} binding energies, adsorption energies, and the experimentally measured in situ X-ray photoelectron spectra of oxygen on silver are reported in an effort to clarify which species are present during ethylene epoxidation. We find that the O_{1s} binding energy of an oxygen adatom increases near linearly with its adsorption energy due to the ionic nature of the Ag/O interaction. Thus, contrary to widespread assignments, a weakly bound oxygen adatom does not account for the electrophilic species with an O_{1s} binding energy of 530 eV that is thought to be active in ethylene epoxidation. Instead, we show that the only species with O_{1s} binding energies near 530 eV are covalently bound, which we find in our calculations, for example, when hydrogen or carbon are present.

KEYWORDS: *silver, oxygen, epoxidation, X-ray photoelectron spectroscopy, density functional theory*
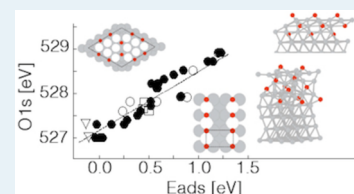
The catalytic epoxidation of ethylene on silver has been of major technological and scientific interest since its discovery in 1931.[1] Although it is accepted that a simple reaction network describes the process—ethylene can react with oxygen to form ethylene oxide (EO) or water and carbon dioxide[1]—this apparent simplicity belies a complex chemistry. Despite decades of study, we lack a lasting understanding of steady-state epoxidation, which has continued to make the Ag/O system an intense area of investigation.[2−6] The challenge has been identifying the active oxygen species under reaction conditions.

Due to thermodynamics, the oxygen species active under steady-state conditions are thought to be weakly bound.[7,8] Thus, it can only be observed at reaction temperatures (500−600 K) by way of in situ techniques.[8] Of these, in situ X-ray photoelectron spectroscopy (XPS) has proven to be an effective tool for the identification of the active species.[4,9] Such studies have revealed that under reaction conditions two types of oxygen are present. The first, nucleophilic oxygen, has an O_{1s} binding energy (BE) of ≈528.5 eV and participates in total combustion; the second, electrophilic oxygen, has an O_{1s} BE of ≈530 eV and participates in epoxidation.[10] Though the atomic structure of nucleophilic oxygen is known,[5] that of electrophilic oxygen remains a mystery, as it is difficult to prepare and study under ultrahigh vacuum (UHV) without severe contamination of the surface.[11] Regardless, the O_{1s} 530 eV feature is usually assigned to unreconstructed adsorbed and/ or dissolved atomic oxygen.[3,12−14] Herein we combine density functional theory (DFT) calculations with in situ measurements to show that, because of the ionic nature of the Ag/O interaction, weakly bound atomic oxygen has an O_{1s} BE less

than 528 eV and cannot account for the electrophilic species thought to be active in steady-state epoxidation.

Previously we have demonstrated that ΔSCF calculations accurately predict O_{1s} BEs in the Ag/O system.[15] Specifically, we confirmed that oxygen in the well-known surface reconstructions on the Ag(110) and Ag(111) surfaces[16,17] gives rise to O_{1s} features consistent with nucleophilic oxygen, 528.1−528.5 eV. The O_{1s} BEs of unreconstructed atomic oxygen on the Ag(111) and Ag(110) surfaces are, however, in the range of 527.0−528.2 eV, whereas oxide-like oxygen appears at 528.6−529.3 eV in the O_{1s} spectrum. All of these BEs are significantly less than that of electrophilic oxygen.

By utilizing a more exhaustive structure space in this work, we show that the calculated O_{1s} BEs of unreconstructed adsorbed atomic oxygen are always *less* than or equal to that of nucleophilic oxygen. This observation holds regardless of surface termination, oxygen adsorption site, the presence of subsurface oxygen, or coverage (see SI for the full comprehensive data). By way of example, the O_{1s} BE of atomic oxygen adsorbed on the 4-fold hollow (FFH) sites of the Ag(100) surface ranges from 527.9 to 528.3 eV for coverages from 1/16−1/2 ML, which is marginally higher than the O_{1s} BE range of 527.1−527.7 eV seen on the Ag(111) over the same range of coverages.[15] We also find that surface/subsurface defects cause only minor (<0.3 eV) variations in these values, whereas introducing subsurface oxygen can increase the computed O_{1s} BE of adsorbed oxygen to 528.9 eV. All of
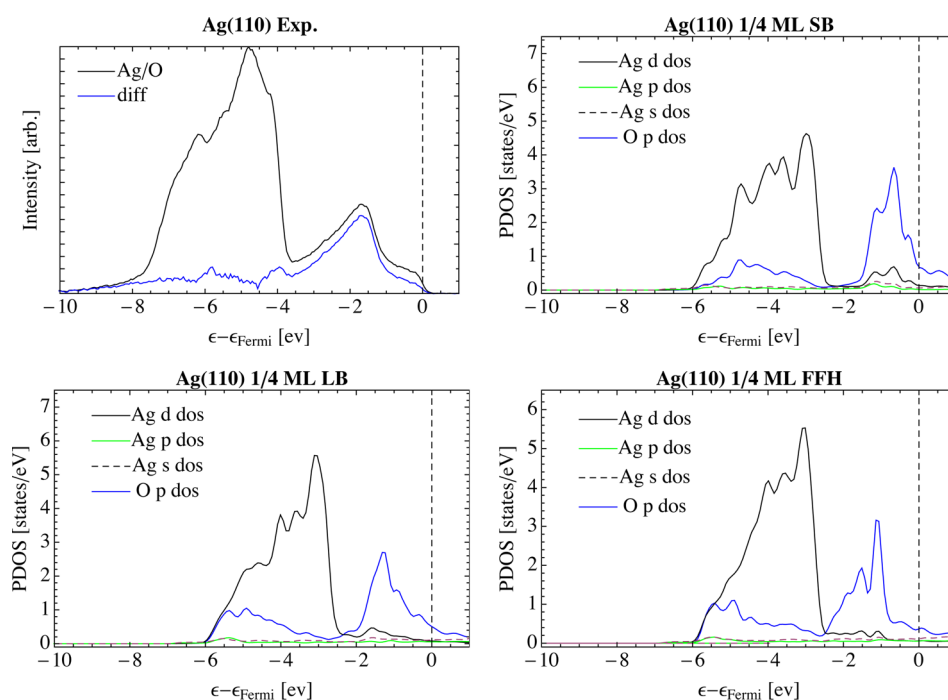
Figure 1. In situ valence band spectrum of a Ag(110) surface under 1×10^{-4} mbar O_2 at 423 K (upper left). The blue curve shows the difference between the in situ spectrum and that of clean silver. Calculated PDOS of oxygen and that of its nearest neighbor silver atom when oxygen is adsorbed on the short bridge (upper right), long bridge (lower left), and 4-fold hollow sites (lower right) on the Ag(110) surface.
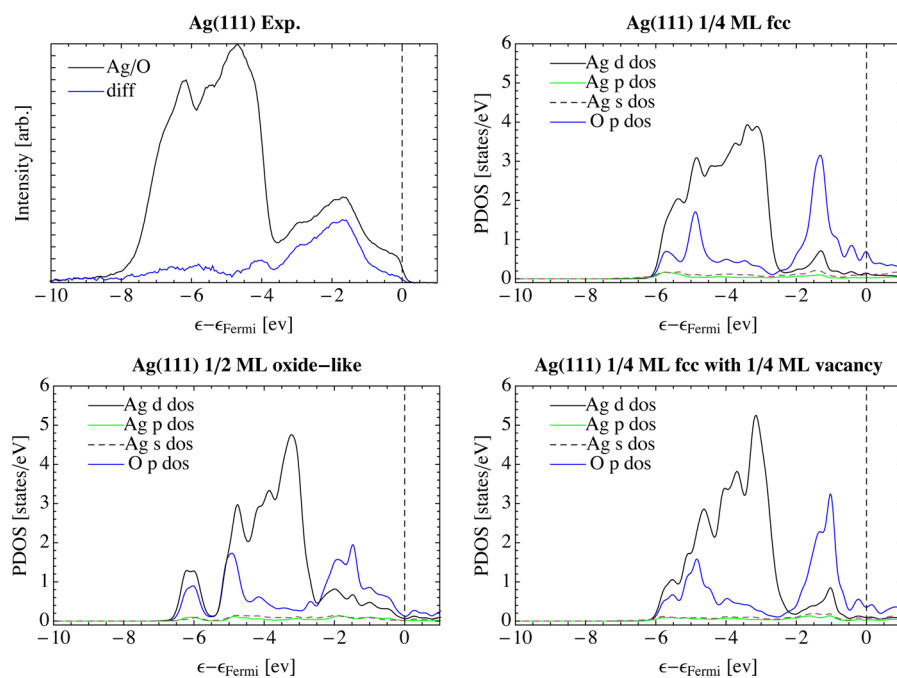

Figure 2. In situ valence band spectrum of a Ag(111) surface under 4×10^{-4} mbar O_2 at 423 K (upper left). The blue curve shows the difference between the in situ spectrum and that of clean silver. Calculated PDOS of oxygen and that of its nearest neighbor silver atom when oxygen is adsorbed on the fcc site (upper right), in an oxide-like layer (lower left), and adjacent to a surface vacancy (lower right) on the Ag(111) surface.

these O_{1s} BEs are well below that of electrophilic oxygen. Furthermore, an increase in O_{1s} BE only occurs with a concomitant increase in the adsorbed species' heat of adsorption, at odds with the widely held view derived from thermodynamic considerations[7] and reaction kinetics[8] that the active oxygen is weakly bound. We now turn to this relationship, the understanding of which is the central result of our work.

Begin by considering how atomic oxygen interacts with a silver surface. It is known that there is some hybridization between O 2p and Ag 4d orbitals, giving rise to a nearly filled Ag/O bonding/antibonding combination, see for instance refs 18 and 19. Electron density differences and the large change in work function associated with oxygen adsorption have been used to demonstrate that the resultant Ag/O interaction is strongly ionic.[18,19] The same is true for the systems we

examined. Take for instance the upper left panel of Figure 1. It shows the in situ valence band spectrum (VB) of a Ag(110) surface with the Fermi energy set to zero. The black line shows the spectrum obtained after exposing the surface to 1×10^{-4} mbar O_2 at 423 K for 20 min to generate nucleophilic oxygen, O_{1s} 528.3 eV (see SI Section III for O_{1s} spectrum). The blue line shows the difference between this in situ spectrum and that measured for the clean surface under UHV. The difference plot was generated by normalizing both spectra to their most intense feature after background subtraction. Oxygen adsorption introduces states above the silver d-band, at ≈ 2 eV below the Fermi energy, along with features inside the silver d-band. These two groups of states correspond to Ag/O antibonding and bonding combinations of O 2p and Ag 4d states, respectively.[18,19]

While a high coverage of unreconstructed atomic oxygen cannot be prepared under controlled conditions, our calculations predict that, on the Ag(110) surface, unreconstructed atomic oxygen interacts with silver in a similar fashion as oxygen in the surface reconstructions, regardless of adsorption site. The lower left panel of Figure 1, for instance, shows the projected density of states (PDOS) of 1/4 ML oxygen adsorbed on the Ag(110) long bridge (LB) site and that of its nearest neighbor silver atom. The blue solid line shows O 2p, the black solid line Ag 4d, the green solid line Ag 5p, and the black dashed line Ag 5s states. Like in the measured spectrum, the interaction between oxygen and silver gives rise to bonding and antibonding states that are both populated. The same behavior can be seen when 1/4 ML oxygen is adsorbed on the short bride (SB) or 4-fold hollow (FFH) sites.

Changing the crystal surface and introducing subsurface oxygen or defects has little effect on this general behavior, see Figure 2. The upper left panel shows the measured VB spectrum of an Ag(111) surface under 4×10^{-4} mbar O_2 pressure at 423 K, conditions under which nucleophilic oxygen forms with a measured O_{1s} BE of 528.2 eV.[15] As before, the blue line shows the difference between the in situ spectrum and that measured for the clean surface under UHV. The Ag/O bonding in this case is analogous to what was observed on the Ag(110) surface. The same can be seen for unreconstructed atomic oxygen on the pristine Ag(111) surface by examining the computed PDOS in the upper right panel of Figure 2. Introducing a surface vacancy or subsurface oxygen does not significantly alter the bonding.[18]

The previous examples indicate that differences in surface, adsorption site, coverage, subsurface oxygen, and defects appear in large part as shifts in the positions of the bonding and antibonding Ag/O states.[18,20] These shifts will alter both the O_{1s} BE and the charge on the adsorbed oxygen. Figure 3 shows

the computed O_{1s} BEs of oxygen on the Ag(110) and Ag(111) surfaces, including oxygen at vacancies and the step edge, plotted against the net Bader charge[21] on the oxygen. As the net Bader charge drops, leading to a less negatively charged oxygen atom, the O_{1s} BE also drops. Within a simplified electrostatic model, the negative slope in Figure 3 is caused by the fact that the interatomic potential contribution to the core level shift changes more quickly than the charge on oxygen.[22] This can be seen by writing the O_{1s} BE shift as

$$\Delta O_{1s} = kq_O + \sum_{i \neq O} q_i/R_{iO} \tag{1}$$

where k is the Coulomb repulsion integral between core and valence states, q_O is the charge on the ionized oxygen, O, q_i are the charges on the remaining atoms in the system, and R_{iO} is the distance between the ith atom and the ionized oxygen. The sum, which runs over all the nuclei except the ionized oxygen, gives the interatomic potential contribution to the core level shift.

Importantly, because the Ag/O bonding is strongly ionic, the relationship between the oxygen charge and its O_{1s} BE seen in Figure 3 is mirrored in oxygen adsorption energies. That is, as the Ag−O bond weakens less charge is transferred from silver to oxygen and the O_{1s} BE is reduced. To use this relationship, we first define the adsorption energy as

$$E_{ads} = -1/N \left[E_{Ag/O} - E_{Ag} - N\frac{1}{2}E_{O_2} \right] \tag{2}$$

where E_{Ag} is the energy of the silver surface, $E_{Ag/O}$ is the energy of the same surface with N oxygen adatoms, and E_{O_2} is the energy of an isolated O_2 molecule computed at the Γ point using a $(40 \times 40 \times 40)$ Bohr box. The adsorption energy is simply the energy gained or lost when an oxygen atom, from O_2, adsorbs on the surface. We have defined it such that a positive (negative) E_{ads} corresponds to exothermic (endothermic) adsorption with respect to gas phase O_2.

With this definition, an oxygen adatom's O_{1s} BE can be seen to scale almost linearly with its E_{ads}, see Figure 4. This
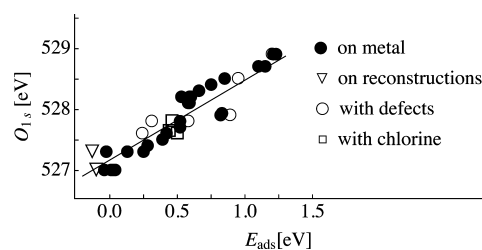
Figure 4. Computed O_{1s} BE of adsorbed oxygen versus adsorption energy, where a positive number indicates exothermic adsorption.

observation suggests that when Ag/O bonding is ionic, weakly bound oxygen, as is postulated to be active in epoxidation, will have a low O_{1s} BE. Thus, it cannot account for the electrophilic species giving rise to an O_{1s} feature at 530 eV.

To test if this scaling holds over a wider range of systems , we considered the effect of coadsorbed chlorine, as well as oxygen on the surface of Ag_2O, and oxygen adatoms on the well-known surface reconstructions. These were chosen because chlorine is known to increase the ratio of electrophilic to nucleophilic oxygen on silver surfaces,[4,23] and the latter two systems have
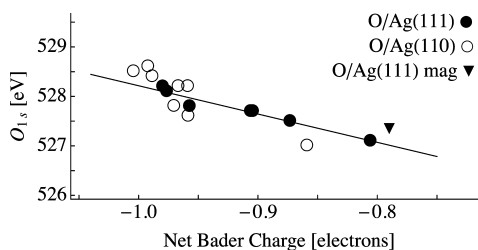

Figure 3. Computed O_{1s} binding energy plotted against the net Bader charge on silver. For 1/2 ML O on the Ag(111) surface, both the magnetic and nonmagnetic solutions are shown.

been suggested as possible candidates for electrophilic oxygen.[6,8]

Coadsorption of chlorine with oxygen fails to alter the scaling relationship or give rise to an O_{1s} BE near 530 eV. When 1/16 and 1/8 ML of chlorine are coadsorbed on the fcc hollow sites of a Ag(111) surface with 1/16 and 1/8 ML coadsorbed oxygen on the fcc hollow sites the computed O_{1s} BE is in the range 527.6−527.8 eV, as compared to 527.6−527.7 eV for 1/16−1/4 ML pure atomic oxygen. Though these coverages of chlorine do little to alter the O_{1s} BE of atomic oxygen, the presence of Ag_2O and surface reconstruction have a profound effect.

Oxygen adsorbed on Ag_2O and oxygen reconstructed surfaces have among the lowest O_{1s} BEs of all the species we investigated, as low as 526.9 eV for an oxygen terminated $Ag_2O(001)$ surface.[15] The O_{1s} BE computed for an additional 1/8 ML oxygen on the $p(4 \times 4)$ reconstruction on the Ag(111) surface is nearly equivalent to those on the $Ag_2O(001)$ surface, 527.0 eV, in contrast to the 528.1 eV computed for the oxygen atoms in the pristine reconstruction. Similarly, the O_{1s} BE of 1/4 ML additional oxygen adsorbed on the FFH sites of the $p(2 \times 1)$ reconstruction on the Ag(110) surface is 527.3 eV (see SI section IIIE for atomic structures). Despite the large changes, these exotic systems tend to follow the scaling behavior shown in Figure 4, with O_{1s} BEs far below that of electrophilic oxygen.

The scaling behavior seen in Figure 4, along with its origin in the ionicity of the Ag/O interaction, demonstrates that oxygen atoms with a high O_{1s} BE cannot account for electrophilic oxygen when they are ionically bound to silver. Take for example the O_γ species with an O_{1s} BE of 529.5−529.7 eV previously observed in some studies.[23,24] Work function measurements of O_γ suggest the Ag/O interaction is strongly ionic.[25] Therefore, we expect the scaling behavior seen in Figure 4 to hold for O_γ, resulting in an estimated adsorption energy of 1.8−1.9 eV/O and a corresponding desorption temperature of 1100−1200 K, calculated using the Redhead equation[26] with a heating rate of 1 K/s and a prefactor of 10^{15} s^{-1}.[27] While this estimated desorption temperature is in good agreement with the measured 900−1100 K,[24,25] O_γ is bound too strongly to account for electrophilic oxygen,[7,8] as are other ionically bound species with an O_{1s} BE near 530 eV.

The types of weakly bound oxygen that may give rise to the O_{1s} feature attributed to electrophilic oxygen are covalently bound. Adsorbed carbonates, for instance, have an O_{1s} BE of approximately 530 eV,[28] though these can be dismissed owing to the absence of a C_{1s} signal during epoxidation.[4] Similarly, the computed O_{1s} BE of 1/4 ML OH adsorbed on the Ag(111) surface is 530.0 eV. The challenge is now to understand if electrophilic oxygen is formed by oxygen bonding to some element other than silver or if the silver surface can be modified to bond more covalently with adsorbed oxygen by a mechanism not considered in this study.

In summary, we used in situ VB, XPS, and DFT calculations to show that, on silver surfaces, unreconstructed atom oxygen appears at 527−528 eV in the O_{1s} spectrum. While a low concentration of such species may be present in during epoxidation they cannot account for the oxygen appearing at 530 eV that is thought to be active in ethylene epoxidation at mbar pressures. We also show that the ionic nature of Ag/O bonding gives rise to a scaling relationship between O_{1s} BE and adatom adsorption energy in which the O_{1s} BE drops with oxygen's adsorption energy. This relationship suggests that only covalently bound oxygen species can account for a weakly bound electrophilic oxygen appearing at 530 eV in the O_{1s}

spectrum. These findings suggest we have yet to reach a lasting understanding of one of the most well studied problems in heterogeneous catalysis.

EXPERIMENTAL AND COMPUTATIONAL SECTION

In situ XPS measurements were performed at the near ambient pressure endstation of the ISISS beamline at the BESSY II synchrotron radiation facility of the Helmholtz-Zentrum Berlin. Details about the system can be found in ref 29, and further details of the current experiments are given in the Supporting Information. Briefly, the single crystals used in the experiments were cleaned by repeating cycles of O_2 treatment at 10^{-3} mbar at 423 K for 20 min, Ar sputtering at 1.5 kV for 20 min, and annealing at 673 K in vacuum (5×10^{-8} mbar) for 5 min. We selected appropriate photon energies to measure core-level spectra for different elements using photoelectrons with the same kinetic energy of 150 eV. The binding energy scale for each spectrum was calibrated by the Fermi edge measured with the same photon energy.

Density Functional Theory (DFT) calculations were performed using the Quantum ESPRESSO package[30] with ultrasoft pseudopotentials, and the exchange and correlation potential developed by Perdew, Burke, and Ernzerhof.[31] O_{1s} BEs were computed by way of the ΔSCF method, resulting in an error of ≤0.3 eV. Bader charges were computed using the Bader charge analysis code.[32] Further details are given in the Supporting Information.

ASSOCIATED CONTENT

Ⓢ Supporting Information

The Supporting Information is available free of charge on the ACS Publications website at DOI: 10.1021/acscatal.5b01543.

Full experimental and computational details (PDF)

AUTHOR INFORMATION

Corresponding Author

*E-mail: trjones@fhi-berlin.mpg.de.

Present Address

§Brazilian Synchrotron Light Laboratory, Campinas CEP 13083-970, Brazil

Notes

The authors declare no competing financial interest.

ACKNOWLEDGMENTS

REFERENCES

(1) Rebsdat, S.; Mayer, D. Ethylene Oxide In *Ullmann's Encyclopedia of Industrial Chemistry*; Wiley-VCH: Weinheim, Germany, 2012; pp 547−572.

(2) Böcklein, S.; Günther, S.; Wintterlin, J. *Angew. Chem., Int. Ed.* **2013**, *52*, 5518−5521.

(3) Williams, F. J.; Bird, D. P. C.; Palermo, A.; Santra, A. K.; Lambert, R. M. *J. Am. Chem. Soc.* **2004**, *126*, 8509−8514.

(4) Rocha, T. C. R.; Hävecker, M.; Knop-Gericke, A.; Schlögl, R. *J. Catal.* **2014**, *312*, 12−16.

(5) Schnadt, J.; Knudsen, J.; Hu, X. L.; Michaelides, A.; Vang, R. T.; Reuter, K.; Li, Z.; Lægsgaard, E.; Scheffler, M.; Besenbacher, F. *Phys. Rev. B: Condens. Matter Mater. Phys.* **2009**, *80*, 075424.

(6) Ozbek, M.; Onal, I.; van Santen, R. *J. Catal.* **2011**, *284*, 230−235.

(7) van Santen, R. A.; Kuipers, H. P. C. E. *Adv. Catal.* **1987**, *35*, 265−321.

(8) Stegelmann, C.; Schiødt, N. C.; Campbell, C. T.; Stoltze, P. *J. Catal.* **2004**, *221*, 630−649.

(9) Bukhtiyarov, V. I.; Nizovskii, A. I.; Bluhm, H.; Hävecker, M.; Kleimenov, E.; Knop-Gericke, A.; Schlögl, R. *J. Catal.* **2006**, *238*, 260−269.

(10) Bukhtiyarov, V. I.; Prosvirin, I. P.; Kvon, R. I. *Surf. Sci.* **1994**, *320*, L47−L50.

(11) Campbell, C. T.; Paffett, M. T. *Surf. Sci.* **1984**, *143*, 517−535.

(12) Joyner, R. W.; Roberts, M. W. *Chem. Phys. Lett.* **1979**, *60*, 459−462.

(13) Au, C.-T.; Singh-Boparai, S.; Roberts, M. W.; Joyner, R. W. *J. Chem. Soc., Faraday Trans. 1* **1983**, *79*, 1779−1791.

(14) Bukhtiyarov, V. I.; Kaichev, V. V.; Prosvirin, I. P. *J. Chem. Phys.* **1999**, *111*, 2169−2175.

(15) Jones, T. E.; Rocha, T. C. R.; Knop-Gericke, A.; Stampfl, C.; Schlögl, R.; Piccinin, S. *Phys. Chem. Chem. Phys.* **2015**, *17*, 9288−9312.

(16) Carlisle, C.; Fujimoto, T.; Sim, W.; King, D. *Surf. Sci.* **2000**, *470*, 15−31.

(17) Bare, S. R.; Griffiths, K.; Lennard, W. N.; Tang, H. T. *Surf. Sci.* **1995**, *342*, 185−198.

(18) Li, W.-X.; Stampfl, C.; Scheffler, M. *Phys. Rev. B: Condens. Matter Mater. Phys.* **2003**, *67*, 045408.

(19) Li, W.-X.; Stampfl, C.; Scheffler, M. *Phys. Rev. B: Condens. Matter Mater. Phys.* **2002**, *65*, 075407.

(20) Jones, T. E.; Rocha, T. C. R.; Knop-Gericke, A.; Stampfl, C.; Schlögl, R.; Piccinin, S. *Phys. Chem. Chem. Phys.* **2014**, *16*, 9002−9014.

(21) Bader, R. F. W. *Atoms in Molecules. A Quantum Theory*; Clarendon Press: Oxford, 1990.

(22) Bagus, P. S.; Illas, F.; Pacchioni, G.; Parmigiani, F. *J. Electron Spectrosc. Relat. Phenom.* **1999**, *100*, 215−236.

(23) Rocha, T. C. R.; Oestereich, A.; Demidov, D. V.; Hävecker, M.; Zafeiratos, S.; Weinberg, G.; Bukhtiyarov, V. I.; Knop-Gericke, A.; Schlögl, R. *Phys. Chem. Chem. Phys.* **2012**, *14*, 4554−4564.

(24) Nagy, A.; Mestl, G.; Herein, D.; Weinberg, G.; Kitzelmann, E.; Schlögl, R. *J. Catal.* **1999**, *182*, 417−429.

(25) Bao, X.; Muhler, M.; Schedel-Niedrig, T.; Schlögl, R. *Phys. Rev. B: Condens. Matter Mater. Phys.* **1996**, *54*, 2249−2262.

(26) Redhead, P. A. *Vacuum* **1962**, *12*, 203−211.

(27) Campbell, C. T. *Surf. Sci.* **1985**, *157*, 43−60.

(28) Knudsen, J.; Martin, N. M.; Grånäs, E.; Blomberg, S.; Gustafson, J.; Andersen, J. N.; Lundgren, E.; Klacar, S.; Hellman, A.; Grönbeck, H. *Phys. Rev. B: Condens. Matter Mater. Phys.* **2011**, *84*, 115430.

(29) Knop-Gericke, A.; Kleimenov, E.; Hävecker, M.; Blume, R.; Teschner, D.; Zafeiratos, S.; Schlögl, R.; Bukhtiyarov, V. I.; Kaichev, V. V.; Prosvirin, I. P.; Nizovskii, A. I.; Bluhm, H.; Barinov, A.; Dudin, P.; Kiskinova, M. *Adv. Catal.* **2009**, *52*, 213−272.

(30) Giannozzi, P.; Baroni, S.; Bonini, N.; Calandra, M.; Car, R.; Cavazzoni, C.; Ceresoli, D.; Chiarotti, G. L.; Cococcioni, M.; Dabo, I.; Dal Corso, A.; de Gironcoli, S.; Fabris, S.; Fratesi, G.; Gebauer, R.; Gerstmann, U.; Gougoussis, C.; Kokalj, A.; Lazzeri, M.; Martin-Samos, L.; Marzari, N.; Mauri, F.; Mazzarello, R.; Paolini, S.; Pasquarello, A.; Paulatto, L.; Sbraccia, C.; Scandolo, S.; Sclauzero, G.; Seitsonen, A. P.; Smogunov, A.; Umari, P.; Wentzcovitch, R. M. *J. Phys.: Condens. Matter* **2009**, *21*, 395502.

(31) Perdew, J. P.; Burke, K.; Ernzerhof, M. *Phys. Rev. Lett.* **1996**, *77*, 3865−3868.

(32) Tang, W.; Sanville, E.; Henkelman, G. *J. Phys.: Condens. Matter* **2009**, *21*, 084204.